Original Article

Wild-type p53-induced Phosphatase 1 Deficiency Exacerbates Myocardial Infarction-induced Ischemic Injury

Ke-Mei Liu[1], Hai-Hong Zhang[2], Ya-Nan Wang[2], Lian-Mei Wang[3], Hong-Yu Chen[2], Cai-Feng Long[2], Lian-Feng Zhang[4], Hong-Bing Zhang[2], Hong-Bing Yan[1]

[1]Department of Coronary Artery Disease, State Key Laboratory of Cardiovascular Disease, Fuwai Hospital, National Center for Cardiovascular Diseases, Chinese Academy of Medical Sciences and Peking Union Medical College, Beijing 100037, China

[2]Department of Physiology, State Key Laboratory of Medical Molecular Biology, Institute of Basic Medical Sciences, Chinese Academy of Medical Sciences and Peking Union Medical College, Beijing 100730, China

[3]Institute of Chinese Materia Medica, China Academy of Chinese Medical Sciences, Beijing 100029, China

[4]Key Laboratory of Human Disease Comparative Medicine, Ministry of Health, Institute of Laboratory Animal Science, Chinese Academy of Medical Sciences and Comparative Medical Center, Peking Union Medical College, Beijing 100021, China

Abstract

Background: Myocardial infarction (MI) is a major disease burden. Wild-type p53-induced phosphatase 1 (Wip1) has been studied extensively in the context of cancer and the regulation of different types of stem cells, but the role of Wip1 in cardiac adaptation to MI is unknown. We investigated the significance of Wip1 in a mouse model of MI.

Methods: The study began in June 2014 and was completed in July 2016. We compared *Wip1*-knockout (*Wip1*-KO) mice and wild-type (WT) mice to determine changes in cardiac function and survival in response to MI. The heart weight/body weight (HW/BW) ratio and cardiac function were measured before MI. Mouse MI was established by ligating the left anterior descending (LAD) coronary artery under 1.5% isoflurane anesthesia. After MI, survival of the mice was observed for 4 weeks. Cardiac function was examined by echocardiography. The HW/BW ratio was analyzed, and cardiac hypertrophy was measured by wheat germ agglutinin staining. Hematoxylin and eosin (H&E) staining was used to determine the infarct size. Gene expression of interleukin-6 (*IL-6*), tumor necrosis factor-α (*TNF-α*), and interleukin-1β (*IL-1β*) was assessed by quantitative real-time polymerase chain reaction (qPCR), and the levels of signal transducers and activators of transcription 3 (stat3) and phosphor-stat3 (p-stat3) were also analyzed by Western blotting. Kaplan-Meier survival analysis, log-rank test, unpaired *t*-test, and one-way analysis of variance (ANOVA) were used for statistical analyses.

Results: *Wip1*-KO mice had a marginally increased HW/BW ratio and slightly impaired cardiac function before LAD ligation. After MI, *Wip1*-deficient mice exhibited increased mortality (57.14% vs. 29.17%; $n = 24$ [WT], $n = 35$ [*Wip1*-KO], $P < 0.05$), increased cardiac hypertrophy (HW/BW ratio: 7 days: 7.25 ± 0.36 vs. 5.84 ± 0.18, $n = 10$, $P < 0.01$, and 4 weeks: 6.05 ± 0.17 vs. 5.87 ± 0.24, $n = 10$, $P > 0.05$; cross-sectional area: 7 days: 311.80 ± 8.29 vs. 268.90 ± 11.15, $n = 6$, $P < 0.05$, and 4 weeks: 308.80 ± 11.26 vs. 317.00 ± 13.55, $n = 6$, $P > 0.05$), and reduced cardiac function (ejection fraction: 7 days: 29.37 ± 1.38 vs. 34.72 ± 1.81, $P < 0.05$, and 4 weeks: 19.06 ± 2.07 vs. 26.37 ± 2.95, $P < 0.05$; fractional shortening: 7 days: 13.72 ± 0.71 vs. 16.50 ± 0.94, $P < 0.05$, and 4 weeks: 8.79 ± 1.00 vs. 12.48 ± 1.48, $P < 0.05$; $n = 10$ [WT], $n = 15$ [*Wip1*-KO]). H&E staining revealed a larger infarct size in *Wip1*-KO mice than in WT mice (34.79% ± 2.44% vs. 19.55% ± 1.48%, $n = 6$, $P < 0.01$). The expression of *IL-6* and p-stat3 was downregulated in *Wip1*-KO mice (IL-6: 1.71 ± 0.27 vs. 4.46 ± 0.79, $n = 6$, $P < 0.01$; and p-stat3/stat3: 1.15 ± 0.15 vs. 1.97 ± 0.23, $n = 6$, $P < 0.05$).

Conclusion: The results suggest that Wip1 could protect the heart from MI-induced ischemic injury.

Key words: Ischemic Injury; Myocardial Infarction; Wild-type p53-induced Phosphatase 1

Introduction

Myocardial infarction (MI) is a major cause of morbidity and mortality worldwide.[1] Once the myocardium is infarcted, a phase associated with irreversible cardiomyocyte apoptosis, fibrosis, inflammation, and hypertrophy occurs.[2,3] MI causes the loss of cardiomyocytes and then followed by proliferation of noncardiomyocytes and induction of

Access this article online

Quick Response Code:

Website: www.cmj.org

DOI: 10.4103/0366-6999.206353

Address for correspondence: Dr. Hong-Bing Yan, Department of Coronary Artery Disease, National Center for Cardiovascular Diseases, Chinese Academy of Medical Sciences and Peking Union Medical College, No. 167, Bei Li Shi Road, Beijing 100037, China
E-Mail: hbyanfuwai@aliyun.com

Received: 11-01-2017 **Edited by:** Peng Lyu
How to cite this article: Liu KM, Zhang HH, Wang YN, Wang LM, Chen HY, Long CF, Zhang LF, Zhang HB, Yan HB. Wild-type p53-induced Phosphatase 1 Deficiency Exacerbates Myocardial Infarction-induced Ischemic Injury. Chin Med J 2017;130:1333-41.

inflammation, which leads to negative cardiac remodeling and heart failure.[4] Although the survival of patients with MI has improved with guideline-directed medical therapy, percutaneous coronary intervention, and coronary artery bypass grafting, the post-MI mortality rate is still high.[5-8] Therefore, it is of great importance to understand the pathological mechanism of MI for the development of novel MI therapeutics.

Type 2C protein phosphatase (PP2C) functions as a monomer with N- and C-terminal extensions that localize enzymes to specific domains and substrates.[9] Wild-type p53-induced phosphatase 1 (Wip1) is a p53-dependent γ or ultraviolet radiation-responsive protein and is also a newly identified member of the PP2C family.[10] Wip1 is also known as protein phosphatase magnesium-dependent 1 delta (PPM1D) because it requires magnesium for its phosphatase activity. The Wip1-encoding gene *PPM1D* is located at human chromosome 17q23 and mouse chromosome 11.[11] Wip1 is overexpressed in numerous human tumors, including breast cancer,[12] medulloblastoma,[13] ovarian cancer,[14,15] gastric carcinoma,[16] pancreatic adenocarcinoma,[17] and chronic lymphocytic leukemia.[18] Recently, Wip1 has also been discovered to play an important role in several physiological processes, such as adult neurogenesis and organismal aging.[19,20] In mouse atherosclerosis models, deficiency of Wip1 results in the inhibition of lipid droplet accumulation in macrophages, prevents the formation of foam cells, and ultimately, suppresses the development of atherosclerotic plaques.[21] Wip1 is highly expressed in the heart,[11] but the role of Wip1 in MI is largely unknown.

In this study, we investigated the role of Wip1 in MI-induced acute and chronic ischemic injury using wild-type (WT) and *Wip1*-knockout (*Wip1*-KO) mice. We found that *Wip1*-KO mice were more susceptible to MI and suffered more severe ischemic injury than WT mice.

Methods

Animals

All animal experiments were performed from June 2014 to July 2016 which were in accordance with the Guidelines for the Care of Experimental Animals Committee of the Chinese Academy of Medical Sciences and Peking Union Medical College, which were based on the National Institutes of Health (NIH) guidelines (Guide for the Care and Use of Laboratory Animals) and the guidelines from Directive 2010/63/EU of the European Parliament on the protection of animals used for scientific purposes. The protocol was approved by the Ethics Committee for Animal Research of Fuwai Hospital (No. 2013-6-6-YJSH) and the mice license is SCXK (Beijing) 2013-0002. C57BL/6 mice were purchased from Vital River Company (Beijing, China). *Wip1*-KO mice were described previously and were backcrossed with C57BL/6 mice for at least ten generations for this study.[22] The number of mice used for each experiment is listed in Supplement Table 1.

Establishment of the myocardial infarction model

MI was established by permanent ligation of the left anterior descending (LAD) coronary artery as previously described.[23] Briefly, WT male mice and *Wip1*-KO male mice (10–12 weeks old) were anesthetized and ventilated with 80% oxygen containing 1.5% isoflurane (Merck, Darmstadt, Germany). A left thoracotomy was performed through the 4th left intercostal space. The left coronary artery was then ligated approximately 2–3 mm away from the tip of the left auricle with a 7-0 silk suture. MI was confirmed by the discoloration of the ventricle. The control mice were subjected to sham surgery without the ligation of a placed suture. The chest and skin were then closed with 4-0 silk sutures.

Echocardiography

Transthoracic echocardiography was conducted in mice before the operation, as well as 7 days and 4 weeks after surgery, using the Vevo 2100 imaging system (VisualSonics Inc., Toronto, Ontario, Canada) with a 30-MHz central frequency scan head. The mice were anesthetized with 1.0–2.0% isoflurane (Merck, Darmstadt, Germany) and placed on a heating pad to maintain body temperature. To allow for consistent measurements at the same anatomic locations in different mice, the left ventricular (LV) dimensions were evaluated using digitally recorded two-dimensional short-axis M-mode tracings at the level of the papillary muscles for at least three consecutive heartbeats. The LV internal diameter at end-diastole (LVIDd), the LV internal diameter at end-systole (LVIDs), and the LV posterior wall thickness at end-diastole (LVPWd) were measured, and the LV ejection fraction (EF) and the LV fractional shortening (FS) were calculated.

Quantitative real-time polymerase chain reaction analysis

RNA was extracted from heart tissues with the Total RNA Kit (OMEGA, Norcross, GA, USA). cDNA synthesis was performed with an oligo-dT primer (TOYOBO, Osaka, Japan) according to the manufacturer's instructions in a reaction volume of 20 μl. For quantitative mRNA analysis, a template equivalent to 20 ng of RNA was subjected to 40 cycles of quantitative real-time polymerase chain reaction (qPCR) using a CFX real-time PCR instrument (Bio-Rad, Hercules, CA, USA) with SYBR Green PCR Master Mix (TransGen, Beijing, China) in triplicate. GAPDH was used for normalization. Relative mRNA expression was calculated using the $2^{-\Delta\Delta Ct}$ method. The primer sequences (forward and reverse) of mouse *Wip1*, collagen I, interleukin-6 (*IL-6*), tumor necrosis factor-α (*TNF-α*), interleukin-1β (*IL-1β*), and *GAPDH* were as follows:

Wip1 (forward 5'-CTGACTGATAGCCCTACTTAC AACA-3' and reverse 5'-GAGAAGGCATTACTGC GAACA-3');

Collagen I (forward 5'-GAGCGGAGAGTACTGGATCG-3' and reverse 5'-TACTCGAACGGGAATCCATC-3');

IL-6 (forward 5'-TCCAGTTGCCTTCTTGGGACTGAT-3' and reverse 5'-TAAGCCTCCGACTTGTGAAGTGGT-3');

TNF-α (forward 5'-TTCCGAATTCACTGGAGCCTCGAA-3' and reverse 5'-TGCACCTCAGGGAAGAATCTGGAA-3');

IL-1β (forward 5'-TGGAGAGTGTGGATCCCAAGCAAT-3' and reverse 5'-TGCTTGTGAGGTGCTGATGTACCA-3'); and

GAPDH (forward 5'-AACTTTGGCATTGTGGAAGG-3' and reverse 5'-ACACATTGGGGGTAGGAACA-3').

Western blotting

Heart tissues were homogenized, and protein was extracted with lysis buffer (2% SDS, 0.1 mol/L DTT, 60 mmol/L, Tris pH 6.8, and 10% glycerol). The samples were then resolved in 4–12% Bis-Tris Ready Gels (Invitrogen, Temecula, CA, USA). Proteins were subsequently transferred to polyvinylidene fluoride (PVDF) membranes (Millipore, Billerica, MA, USA) and then blocked for 1 h at room temperature in phosphate-buffered saline (PBS) containing 0.1% Tween-20 (PBST) and 5% dry nonfat milk. The PVDF membranes were incubated overnight with the following primary antibodies: anti-signal transducers and activators of transcription 3 (stat3) and phosphor-stat3 (Tyr705) (p-stat3) (rabbit polyclonal, 1:1000 dilution; Cell Signaling Technology, Danvers, MA, USA), followed by incubation with the appropriate secondary antibody. Immunoreactive bands were visualized using an enhanced chemiluminescence substrate from Thermo-Fisher Scientific (Waltham, MA, USA). The signals of the detected proteins were quantified with the ImageJ software (NIH, Bethesda, Maryland, USA) and further standardized to the corresponding stat3 value by densitometric analysis.

Tissue fixation and histological analysis

Four weeks after coronary ligation, the mice were anesthetized with 5% isoflurane (Merck, Darmstadt, Germany) and 95% oxygen in a gas chamber. The hearts of the mice were harvested and fixed for 24 h in 4% paraformaldehyde at room temperature, dehydrated using increasing concentrations of ethanol, embedded in paraffin, and sectioned at a thickness of 3 μm from the portion approximately 400 μm distal to the ligation point. Samples were stained with hematoxylin and eosin (H&E) for the detection of infarct size. Photomicrographs were obtained using an Olympus microscope (Tokyo, Japan), and the areas were measured using the ImageJ software (NIH). The infarct size was calculated as a percentage of the LV area. Wheat germ agglutinin (WGA) staining was carried out using immunofluorescence staining to measure cell size. Photomicrographs were obtained using a ZEISS microscope (Oberkochen, Germany). Suitable cross-sections with nearly circular to oval cardiomyocyte sections were selected. The outlines of the cardiomyocytes were traced using the ImageJ software (NIH) to determine the cardiomyocyte cross-sectional area. A value was calculated by the measurement of 400–600 cells in an area remote from the infarct of each heart. Tissue sections were stained with Masson's trichrome to evaluate cardiac fibrosis after MI.

Statistical analysis

Data are expressed as mean ± standard error (SE). The overall survival rate was determined using Kaplan-Meier survival analysis and compared by the log-rank test. Comparisons between two groups were performed using unpaired *t*-tests. One-way analysis of variance (ANOVA) was used for multiple comparisons. Differences were considered statistically significant when the calculated (two-tailed) $P < 0.05$. All analyses were performed using GraphPad Prism 5 (GraphPad Software, La Jolla, CA, USA).

Results

Knockout of wild-type p53-induced phosphatase 1 impairs cardiac function in mice

To explore the physiological role of Wip1 in the mouse heart, we first generated *Wip1*-KO mice [Figure 1a]. qPCR analysis revealed diminished *Wip1* mRNA levels in *Wip1*-KO mouse hearts [0.05 ± 0.01 vs. 0.87 ± 0.09, $n = 6$; Figure 1b]. Reliable antibodies against Wip1 were not available for the demonstration of *Wip1* deficiency. The EF and FS were decreased in *Wip1*-KO mice [EF: 57.48 ± 1.25 vs. 63.76 ± 1.90, FS: 29.96 ± 0.87 vs. 34.29 ± 1.36; $n = 10$–15; Table 1]. Therefore, deletion of *Wip1* causes mild cardiac dysfunction in mice.

Wild-type p53-induced phosphatase 1 deficiency increases myocardial infarction-induced cardiac dysfunction, cardiac hypertrophy, and mortality

To determine whether the status of Wip1 influences the severity of ischemic injury induced by MI, WT and *Wip1*-KO mice were subjected to permanent LAD coronary artery ligation. The mice were followed for 4 weeks after the operation. Most of the mice died on the 1st day after MI, and all of the deaths occurred within 7 days after MI. Among all of the mice, approximately 63% had cardiac rupture. The mortality rate of *Wip1*-KO mice was as high as 57.14%, while the mortality rate of WT mice was 29.17% after MI; none of the sham-ligated WT or *Wip1*-KO mice died [57.14% vs. 29.17% $n = 8$–35; Figure 2a]. Echocardiographic investigations were carried out in the remaining mice whose hearts presumably suffered less damage than the deceased mice. A difference in heart rate was not observed between the *Wip1*-KO and WT mice [475.8 ± 5.1 vs. 453.6 ± 17.3; $n = 10$–15; Table 1]. EF and FS were significantly decreased in *Wip1*-KO mice compared with WT mice both 7 days and 4 weeks after MI [EF: 7 days: 29.37 ± 1.38 vs. 34.72 ± 1.81, and 4 weeks: 19.06 ± 2.07 vs. 26.37 ± 2.95; FS: 7 days: 13.72 ± 0.71 vs. 16.50 ± 0.94, and 4 weeks: 8.79 ± 1.00 vs. 12.48 ± 1.48; $n = 10$–15; Table 1 and Figure 2b–2d]. To evaluate the infarct size of mice, H&E staining of heart tissues was performed 4 weeks after MI. The infarct size was significantly larger in *Wip1*-KO mice than in WT mice [34.79% ± 2.44% vs.19.55% ± 1.48%; $n = 6$; Figure 3a and 3b]. The heart weight/body weight (HW/BW) ratio was calculated, and WGA staining was assessed to investigate cardiac hypertrophy after MI surgery. Although the HW/BW ratio in *Wip1*-KO mice was higher than that in WT mice before MI, the HW and HW/BW ratio increased in *Wip1*-KO

mice compared with WT mice 7 days after MI and returned to the same levels 4 weeks after MI [HW/BW ratio: 7 days: 7.25 ± 0.36 vs. 5.84 ± 0.18, and 4 weeks: 6.05±0.17 vs. 5.87 ± 0.24; $n = 10$; Figure 4a–4c]. WGA staining showed that the cardiomyocyte cell size of *Wip1*-KO mice was much larger than that of WT mice 7 days after MI, while there was no significant difference between the two groups 4 weeks after MI [7 days: 311.80 ± 8.29 vs. 268.90 ± 11.15, and 4 weeks: 308.80 ± 11.26 vs. 317.00 ± 13.55; $n = 6$; Figure 4d and 4e]. Masson's trichrome staining and the expression of collagen I mRNA were assessed to detect cardiac fibrosis after MI. Although cardiac fibrosis was significantly increased due to MI, there was no significant difference in fibrosis between *Wip1*-KO mice and WT mice 4 weeks after MI [3.29 ± 0.48 vs. 2.73 ± 0.29; $n = 6$; Figure 5a and 5b]. Therefore, we reasoned that Wip1 plays a protective role in MI.

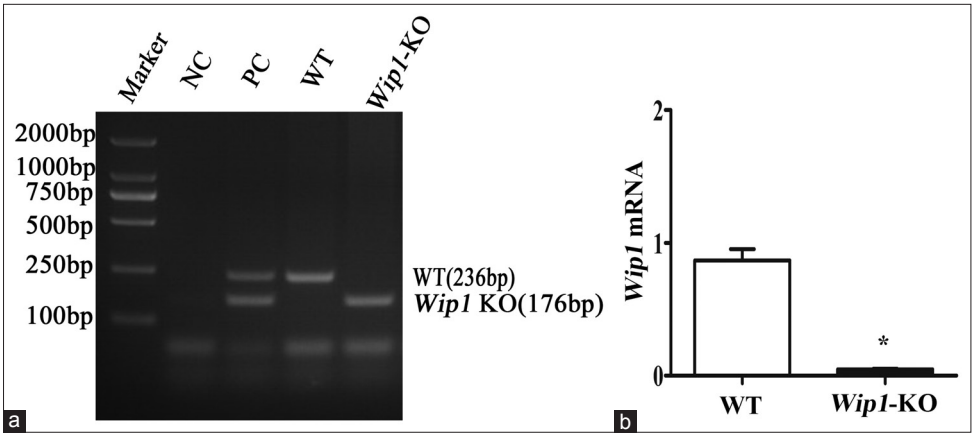

Figure 1: *Wip*1 deficiency mildly impairs cardiac function. (a) Genotyping results for cardiac tissues from WT and *Wip1*-KO mice. (b) *Wip1* mRNA expression in WT mice and *Wip1*-KO mice ($n = 6$ per group). *$P < 0.001$. Data are expressed as the mean ± standard error. NC: Negative control; PC: Positive control; WT: Wild-type mice; *Wip1*: Wild-type p53-induced phosphatase 1; KO: Knockout; *Wip1*-KO: *Wip1*-knockout mice.

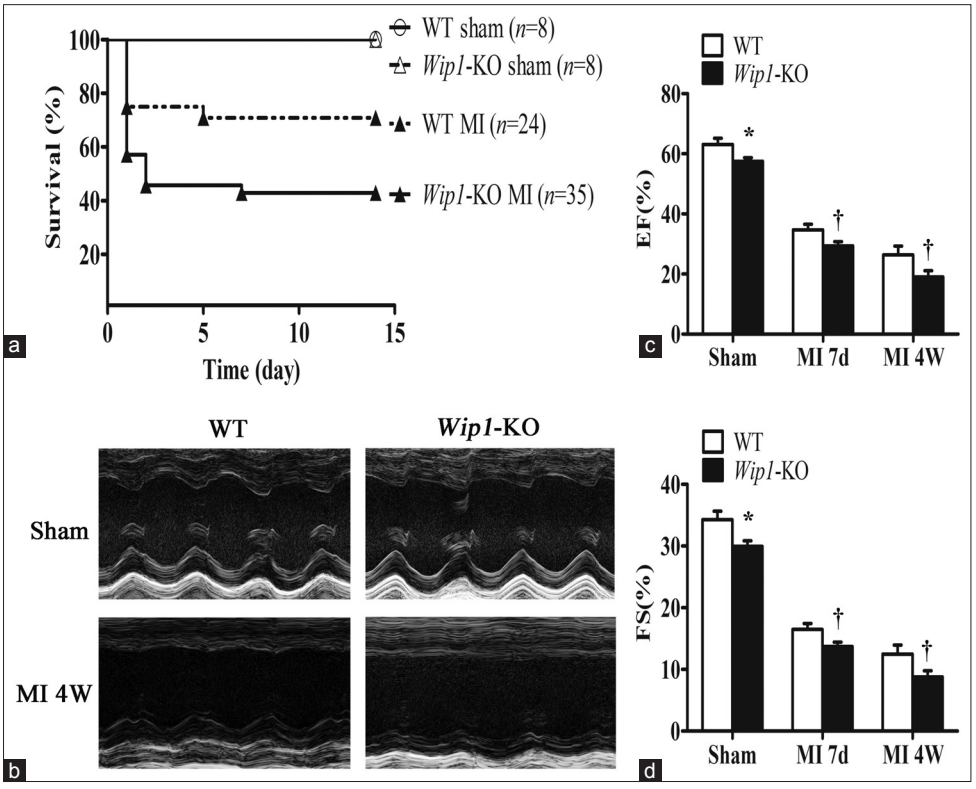

Figure 2: Deletion of *Wip1* increases mortality and promotes cardiac dysfunction after MI. (a) Kaplan-Meier survival curves of mice in the four groups. Statistical analyses were performed using the log-rank test. (b) Representative M-mode echocardiograms of WT mice and *Wip1*-KO mice including graphs from sham mice (top) and the survived mice at 4 weeks after MI (bottom). (c and d) EF and FS were measured in sham- and MI-operated WT mice ($n = 10$ per group) and *Wip1*-KO mice ($n = 15$ per group) at 7 days and 4 weeks after MI. *$P < 0.01$, and †$P < 0.05$. Data are expressed as the mean ± standard error. WT: Wild-type mice; *Wip1*-KO: Wild-type p53-induced phosphatase 1-knockout mice; MI: Myocardial infarction; EF: Ejection fraction; FS: Fractional shortening.

Table 1: Echocardiographic parameters of *Wip1*-KO mice and WT mice before and after myocardial infarction

Parameters	WT (n = 10)			*Wip1*-KO (n = 15)			MI 7 days		MI 4 weeks	
	Preoperation	MI 7 days	MI 4 weeks	Preoperation	MI 7 days	MI 4 weeks	t	P	t	P
Heart rate (beats/min)	453.60 ± 17.31	444.90 ± 18.85	471.90 ± 12.08	475.80 ± 5.10	452.40 ± 13.21	451.70 ± 12.74	0.33	0.741	1.09	0.289
LVIDd (mm)	3.90 ± 0.09	4.42 ± 0.14	5.46 ± 0.16	4.13 ± 0.09	4.42 ± 0.14	5.36 ± 0.14	0.01	0.992	0.43	0.669
LVIDs (mm)	2.56 ± 0.08	3.70 ± 0.15	4.78 ± 0.19	2.90 ± 0.09	3.82 ± 0.13	4.90 ± 0.16	0.61	0.550	0.48	0.637
LVPWd (mm)	0.64 ± 0.04	0.67 ± 0.05	0.57 ± 0.09	0.69 ± 0.03	0.58 ± 0.06	0.54 ± 0.06	1.05	0.304	0.27	0.789
EF (%)	63.76 ± 1.90	34.72 ± 1.81	26.37 ± 2.95	57.48 ± 1.25	29.37 ± 1.38	19.06 ± 2.07	2.38	0.026*	2.09	0.048*
FS (%)	34.29 ± 1.36	16.50 ± 0.94	12.48 ± 1.48	29.96 ± 0.87	13.72 ± 0.71	8.79 ± 1.00	2.40	0.025*	2.15	0.042*

*The *Wip1*-KO group versus the WT group. Data are expressed as the mean ± SE. LVIDd: Left ventricular internal diameter at end-diastole; LVIDs: Left ventricular internal diameter at end-systole; LVPWd: Left ventricular posterior wall thickness at end-diastole; EF: Ejection fraction; FS: Fractional shortening; *Wip1*-KO: Wild-type p53-induced phosphatase 1-knockout mice; WT: Wild-type mice; SE: Standard error; MI: Myocardial infarction.

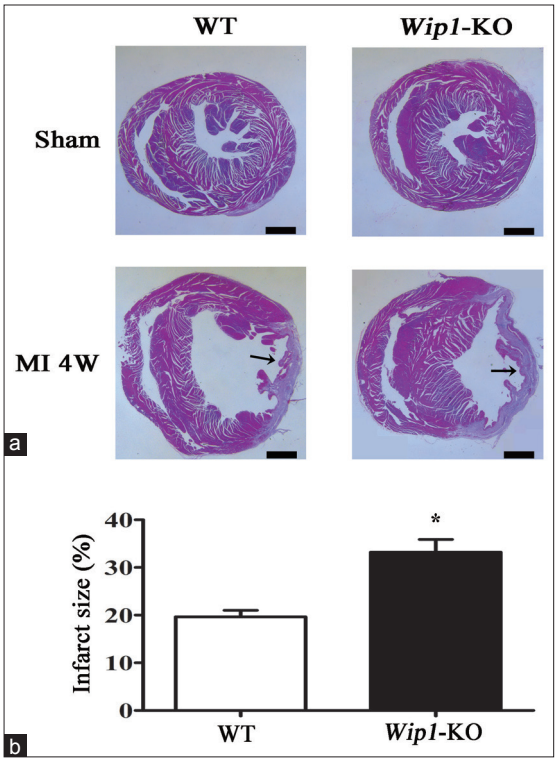

Figure 3: *Wip1* deficiency increases myocardial infarct size following MI. (a) Representative Hematoxylin and eosin staining of heart tissues from sham- and MI-operated WT mice and *Wip1*-KO mice at 4 weeks after MI (n = 6 per group). The arrows refer to the infarcted myocardium. (b) Quantitative analysis of infarct size in WT mice and *Wip1*-KO mice at 4 weeks after MI (n = 6 per group). *P < 0.01. Data are expressed as the mean ± standard error. Scale bar = 1000 μm. WT: Wild-type mice; *Wip1*-KO: Wild-type p53-induced phosphatase 1-knockout mice; MI: Myocardial infarction.

Deletion of wild-type p53-induced phosphatase 1 blocks the myocardial infarction-induced expression of inflammatory cytokines and decreases the level of phosphor-signal transducers and activators of transcription 3

Because most of the deaths occurred on the 1st day after MI, we speculated that Wip1 might alleviate the acute ischemic injury induced by MI. On the 1st day after MI, the mortality rate of *Wip1*-KO mice was 42.85% while that of WT mice was only 25.0%. Inflammation is believed to be a crucial determinant of myocardial healing, and the inflammatory response during the acute postinfarct period is protective.[23] Using qPCR, we checked the expression of inflammatory cytokines, including *IL-6*, *TNF-α*, and *IL-1β*, in the infarcted areas. The level of *IL-6* mRNA in *Wip1*-KO mice was decreased compared with that in WT mice 1 day after MI [1.71 ± 0.27 vs. 4.46 ± 0.79, n = 6; Figure 6a]. Although MI-induced mRNA expression of *TNF-α* and *IL-1β* was compromised in *Wip1*-KO mice, the changes were not statistically significant [*TNF-α*: 2.38 ± 0.39 vs. 4.40 ± 1.46, *IL-1β*: 3.38 ± 0.49 vs. 4.91 ± 1.05; n = 6; Figure 6b and 6c]. Heart tissues of infarcted mice were immunoblotted one day after MI. Although phosphorylation of stat3 was significantly increased by coronary ligation, stat3 was less activated in *Wip1*-KO mice than that in WT mice [1.15 ± 0.15 vs. 1.97 ± 0.23, n = 6; Figure 6d and 6e]. Therefore, *Wip1* depletion blunted the MI-mediated expression of inflammatory cytokines and reduced the level of p-stat3.

Discussion

We demonstrated in this study that Wip1 is critically involved in MI-mediated ischemic injury. We observed a slightly higher HW/BW ratio and impaired cardiac function in *Wip1*-KO mice compared with WT mice before MI. *Wip1* deficiency in mice impairs cardiac function and increases mortality due to augmented acute ischemic injury and increased myocardial infarct size after MI.

Wip1 has been implicated in physiological homeostasis and several human diseases.[24] By suppressing the expression of multiple tumor suppressors, including p53, p38 MAP kinase, and ataxia telangiectasia-mutated signals, *Wip1* functions as an oncogene.[25] The expression of *Wip1* mRNA diminishes with age.[26] Overexpression of *Wip1* may rescue age-related reduction in proliferation and regenerative capacity.[20] *Wip1*-deficient mice exhibit a variety of postnatal abnormalities, including decreased male body mass, male reproductive organ atrophy, reduced male longevity, increased susceptibility to infections, and diminished T- and B-cell function.[22] Consistent with the findings of previous studies, the body weight of *Wip1*-KO male mice was lower than that of WT male mice in the present study. *Wip1*-KO mice had increased HW/BW ratios and cardiac dysfunction compared with WT mice. As there is no significant

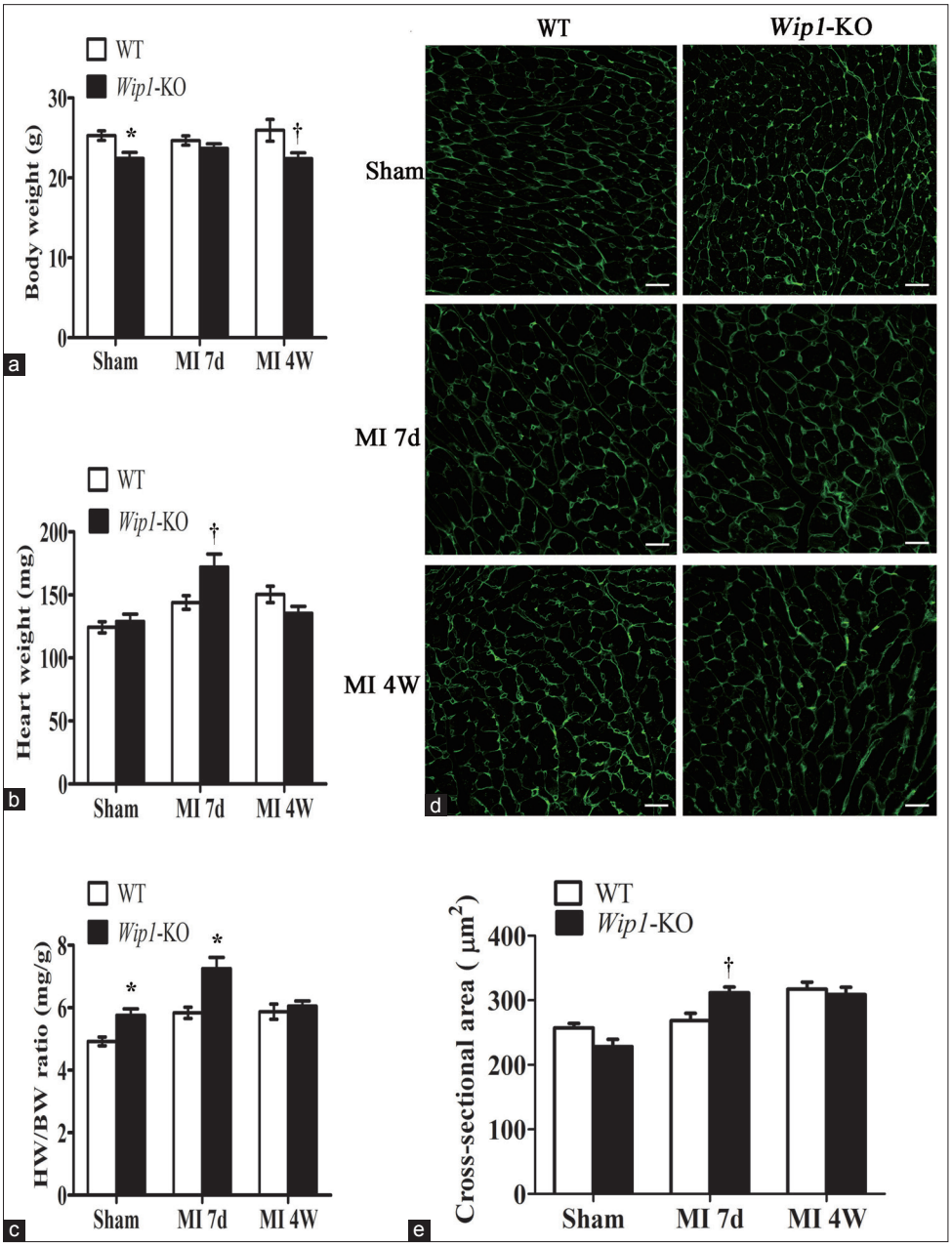

Figure 4: *Wip1* deficiency increases heart weight, HW/BW ratio, and cardiac hypertrophy after MI. (a–c) The body weight, heart weight, and HW/BW ratio of sham- and MI-operated WT and *Wip1*-KO mice at 7 days and 4 weeks after MI ($n = 10$ per group). *$P < 0.01$, and †$P < 0.05$. (d) Representative images showing wheat germ agglutinin staining of sham- and MI-operated WT and *Wip1*-KO mice at 7 days and 4 weeks after MI. (e) Quantitative analysis of cardiomyocyte cross-sectional area in WT and *Wip1*-KO mice ($n = 6$ per group). †$P < 0.05$. Data are expressed as the mean ± standard error. Scale bar = 20 μm. WT: Wild-type mice; *Wip1*-KO: Wild-type p53-induced phosphatase 1-knockout mice; MI: Myocardial infarction; HW/BW: Heart weight/body weight.

difference between WT mice and *Wip1*-KO mice in cross-sectional area of cardiomyocyte illustrated by WGA staining, the reduced body weight might contribute to the increased HW/BW ratio in *Wip1*-KO mice before MI. Glucose intolerance and insulin resistance may cause lower body weight of *Wip1*-KO mice.[27] Myocardial edema might be the cause of the increased HW/BW ratio and cross-sectional area 7 days after MI in *Wip1*-KO mice. At 4 weeks after MI, the difference of cardiac hypertrophy between two groups of mice disappeared, suggesting late tissue repair in the *Wip1*-KO mice. After LAD ligation, both of the LV anterior wall and posterior wall got thinned. We speculate that the LAD coronary artery supplies not only the LV anterior wall but also the posterior wall. When LAD is ligated, the posterior wall is also affected. To compensate the dysfunctional anterior wall due to MI, the left posterior wall overworked until cardiac decompensation occurs. The LV posterior wall might gradually become thinner due to overload. In the intestinal ischemia/reperfusion (I/R) injury mouse models, *Wip1* deficiency causes more severe intestinal I/R injury.[28] In the present study, we found a similar

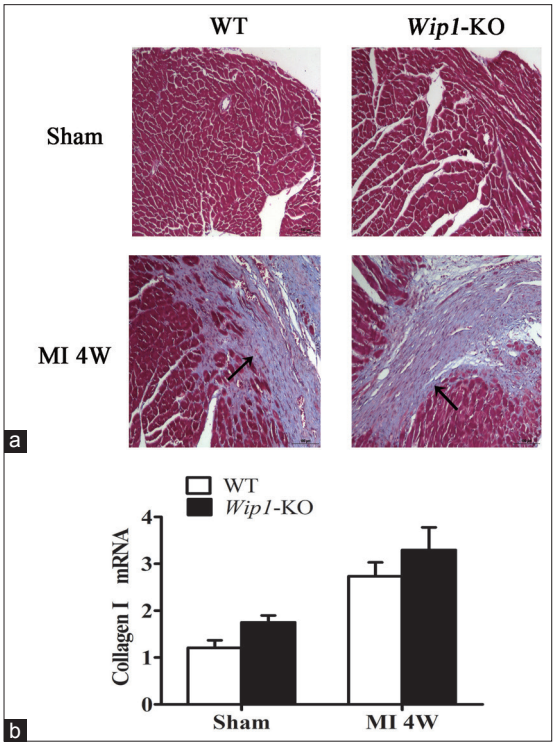

Figure 5: *Wip1* deficiency does not affect cardiac fibrosis after MI. (a) Masson's trichrome staining of heart tissues from sham- and MI-operated WT and *Wip1*-KO mice at 4 weeks after MI (n = 6 per group). The arrows refer to the abundant cardiac fibrosis. (b) qPCR analysis of collagen I mRNA expression at 4 weeks after MI (n = 6 per group). Data are expressed as the mean ± standard error. Scale bar = 100 μm. WT: Wild-type mice; *Wip1*-KO: Wild-type p53-induced phosphatase 1-knockout mice; MI: Myocardial infarction; qPCR: Quantitative real-time polymerase chain reaction.

protective role of Wip1 in mice after MI. The *Wip1*-KO mice exhibited a larger cardiac infarct size, more severe cardiac hypertrophy, poorer cardiac function, and higher mortality than the WT mice after MI. Therefore, Wip1 might limit ischemic injury after MI.

The inflammatory response is activated immediately after MI. Myocardial necrosis triggers inflammatory reactions to heal the wound by removing dead cells and matrix debris and activates reparative pathways that are necessary for scar formation.[29] The release of inflammatory cytokines might contribute to the survival or death of myocytes, modulate cardiac contractility, alter the vascular endothelium, and recruit additional circulating inflammatory cells to the injured myocardium.[30] A proper inflammatory response is thus protective and limits host damage in the acute phase after MI.[31] *Wip1*-KO mice are more susceptible to infection and have a higher frequency of ulcerated skin lesions.[22] In addition, Wip1 was shown to play a critical role in inflammation after genotoxic stress.[32] We noticed that mRNA levels of *IL-6*, *TNF-α*, and *IL-1β* were all significantly increased after MI. Knockout of *Wip1* drastically compromised the MI-induced elevation of *IL-6* and reduced the MI-induced expression of *TNF-α* and *IL-1β* although to a lesser extent.

A previous study showed that IL-6 improves contractile function by enhancing paracrine effects.[33] The lower level of IL-6 in the *Wip1*-KO mice might explain the impaired cardiac function observed after MI. IL-6 activates the intracellular JAK-STAT signaling transduction pathway via a cell surface glycoprotein, gp130.[34] Disturbed gp130 downregulates the

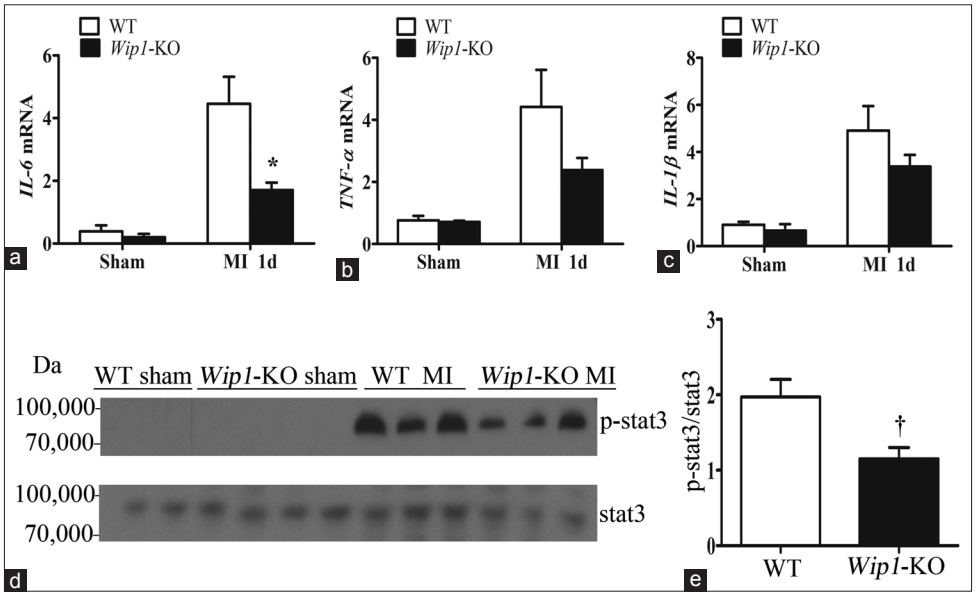

Figure 6: Deletion of *Wip1* inhibits the expression of inflammatory cytokines and p-stat3 after MI. (a–c) qPCR analysis of *IL-6, TNF-α*, and *IL-1β* mRNA expression 1 day after MI (n = 6 per group). *P < 0.01. (d) Representative Western blotting results of p-stat3 and stat3 in sham- and MI-operated WT and *Wip1*-KO mice 1 day after MI (n = 6 per group). stat3 was used as a loading control. (e) Densitometric analysis of the relative level of p-stat3 expression (n = 6 per group). †P < 0.05. Data are expressed as the mean ± standard error. WT: Wild-type mice; *Wip1*-KO: Wild-type p53-induced phosphatase 1-knockout mice; MI: Myocardial infarction; *IL-6*: Interleukin-6; *TNF-α*: Tumor necrosis factor-α; *IL-1β*: Interleukin-1β; qPCR: Quantitative real-time polymerase chain reaction; stat3: Signal transducers and activators of transcription 3; p-stat3: phosphor-stat3.

phosphorylation of stat3, promoting cardiac inflammation and adverse remodeling, which causes heart failure.[35] As a downstream signaling molecule of IL-6, stat3 is also required for preconditioning. The infarct size of preconditioned IL-6 knockout mice is similar to that of WT mice. Reduction of JAK/STAT pathway activity is the main reason for the abrogated infarct-reducing effect.[36] The IL-6-stat3 axis plays a protective role in MI.[35,37] While the IL-6-stat3 signaling cascade was significantly activated by MI in WT mice, *Wip1* deficiency abrogated the MI-induced activation of the IL-6-stat3 signaling pathway. We speculate that Wip1 shields the heart from acute ischemic injury through the activation of IL-6-stat3 signaling. However, elucidation of the relationship between Wip1 and the IL-6-stat3 signaling pathway in Wip1-mediated cardiac protection requires further study.

Even though there is small difference between WT mice and *Wip1*-KO mice before and 7 days or 4 weeks after MI, these marginal differences could not contribute to the 54.3% death of *Wip1*-KO mice versus 25.0% death of WT mice 2 days after MI. They also could not account for the changes of *IL-6* and p-stat3 1 day after MI. Therefore, the statistical analysis of data collected from sham mice and the survived (presumably less severe) mice 7 days or 4 weeks after MI is biased and has limitation. In addition, the molecular mechanism that leads to the aggravation of MI in *Wip1*-KO mice is still unknown. Although the levels of *IL*-6 and p-stat3 were decreased in *Wip*1-KO mice, the relationship between Wip1 and inflammation or the IL-6-stat3 signaling pathway after MI requires further study.

In conclusion, this study provides information on the role of Wip1 in protecting the heart from MI-induced ischemic injury. We suggest that the manipulation of Wip1 might be a novel strategy for the treatment of MI.

Supplementary information is linked to the online version of the paper on the Chinese Medical Journal website.

Acknowledgments

We are grateful to Dr. Pei-He Wang (Fuwai Hospital, Beijing, China) for the kind support in the establishment of the myocardial infarction models and Ms. Qing Xu (Capital Medical University, Beijing, China) for the echocardiographic examinations.

Financial support and sponsorship

This work was supported by the National Natural Science Foundation of China (No. 81270288, and No. 81070167).

Conflicts of interest

There are no conflicts of interest.

References

1. Oliveira GB, Avezum A, Roever L. Cardiovascular disease burden: Evolving knowledge of risk factors in myocardial infarction and stroke through population-based research and perspectives in global prevention. Front Cardiovasc Med 2015;2:32. doi: 10.3389/fcvm.2015.00032.
2. Opie LH, Commerford PJ, Gersh BJ, Pfeffer MA. Controversies in ventricular remodelling. Lancet 2006;367:356-67. doi: 10.1016/S0140-6736(06)68074-4.
3. Sutton MG, Sharpe N. Left ventricular remodeling after myocardial infarction: Pathophysiology and therapy. Circulation 2000;101:2981-8. doi: 10.1161/01.CIR.101.25.2981.
4. Lal H, Zhou J, Ahmad F, Zaka R, Vagnozzi RJ, Decaul M, *et al.* Glycogen synthase kinase-3α limits ischemic injury, cardiac rupture, post-myocardial infarction remodeling and death. Circulation 2012;125:65-75. doi: 10.1161/CIRCULATIONAHA.111.050666.
5. Yeh RW, Sidney S, Chandra M, Sorel M, Selby JV, Go AS. Population trends in the incidence and outcomes of acute myocardial infarction. N Engl J Med 2010;362:2155-65. doi: 10.1056/NEJMoa0908610.
6. McManus DD, Gore J, Yarzebski J, Spencer F, Lessard D, Goldberg RJ. Recent trends in the incidence, treatment, and outcomes of patients with STEMI and NSTEMI. Am J Med 2011;124:40-7. doi: 10.1016/j.amjmed.2010.07.023.
7. Jernberg T, Johanson P, Held C, Svennblad B, Lindbäck J, Wallentin L; SWEDEHEART/RIKS-HIA. Association between adoption of evidence-based treatment and survival for patients with ST-elevation myocardial infarction. JAMA 2011;305:1677-84. doi: 10.1001/jama.2011.522.
8. Zhang B, Shen DP, Zhou XC, Liu J, Huang RC, Wang YE, *et al.* Long-term prognosis of patients with acute non-ST-segment elevation myocardial infarction undergoing different treatment strategies. Chin Med J 2015;128:1026-31. doi: 10.4103/0366-6999.155071.
9. Lammers T, Lavi S. Role of type 2C protein phosphatases in growth regulation and in cellular stress signaling. Crit Rev Biochem Mol Biol 2007;42:586-8. doi: 10.1080/10409230701693342.
10. Fiscella M, Zhang H, Fan S, Sakaguchi K, Shen S, Mercer WE, *et al.* Wip1, a novel human protein phosphatase that is induced in response to ionizing radiation in a p53-dependent manner. Proc Natl Acad Sci U S A 1997;94:6048-53. doi: 10.1073/pnas.94.12.6048.
11. Choi J, Appella E, Donehower LA. The structure and expression of the murine wildtype p53-induced phosphatase 1 (Wip1) gene. Genomics 2000;64:298-306. doi: 10.1006/geno.2000.6134.
12. Li J, Yang Y, Peng Y, Austin RJ, van Eyndhoven WG, Nguyen KC, *et al.* Oncogenic properties of PPM1D located within a breast cancer amplification epicenter at 17q23. Nat Genet 2002;31:133-4. doi: 10.1038/ng888.
13. Castellino RC, De Bortoli M, Lu X, Moon SH, Nguyen TA, Shepard MA, *et al.* Medulloblastomas overexpress the p53-inactivating oncogene WIP1/PPM1D. J Neurooncol 2008;86:245-56. doi: 10.1007/s11060-007-9470-8.
14. Tan DS, Lambros MB, Rayter S, Natrajan R, Vatcheva R, Gao Q, *et al.* PPM1D is a potential therapeutic target in ovarian clear cell carcinomas. Clin Cancer Res 2009;15:2269-80. doi: 10.1158/1078-0432.CCR-08-2403.
15. Yin S, Wang P, Yang L, Liu Y, Wang Y, Liu M, *et al.* Wip1 suppresses ovarian cancer metastasis through the ATM/AKT/Snail mediated signaling. Oncotarget 2016;7:29359-70. doi: 10.18632/oncotarget.8833.
16. Fuku T, Semba S, Yutori H, Yokozaki H. Increased wild-type p53-induced phosphatase 1 (Wip1 or PPM1D) expression correlated with downregulation of checkpoint kinase 2 in human gastric carcinoma. Pathol Int 2007;57:566-71. doi: 10.1111/j.1440-1827.2007.02140.x.
17. Loukopoulos P, Shibata T, Katoh H, Kokubu A, Sakamoto M, Yamazaki K, *et al.* Genome-wide array-based comparative genomic hybridization analysis of pancreatic adenocarcinoma: Identification of genetic indicators that predict patient outcome. Cancer Sci 2007;98:392-400. doi: 10.1111/j.1349-7006.2007.00395.x.
18. López-Guerra M, Trigueros-Motos L, Molina-Arcas M, Villamor N, Casado FJ, Montserrat E, *et al.* Identification of TIGAR in the equilibrative nucleoside transporter 2-mediated response to fludarabine in chronic lymphocytic leukemia cells. Haematologica 2008;93:1843-51. doi: 10.3324/haematol.13186.
19. Zhu YH, Zhang CW, Lu L, Demidov ON, Sun L, Yang L, *et al.* Wip1 regulates the generation of new neural cells in the adult olfactory bulb through p53-dependent cell cycle control. Stem Cells 2009;27:1433-42. doi: 10.1002/stem.65.

20. Wong ES, Le Guezennec X, Demidov ON, Marshall NT, Wang ST, Krishnamurthy J, *et al.* p38MAPK controls expression of multiple cell cycle inhibitors and islet proliferation with advancing age. Dev Cell 2009;17:142-9. doi: 10.1016/j.devcel.2009.05.009.
21. Le Guezennec X, Brichkina A, Huang YF, Kostromina E, Han W, Bulavin DV. Wip1-dependent regulation of autophagy, obesity, and atherosclerosis. Cell Metab 2012;16:68-80. doi: 10.1016/j.cmet.2012.06.003.
22. Choi J, Nannenga B, Demidov ON, Bulavin DV, Cooney A, Brayton C, *et al*. Mice deficient for the wild-type p53-induced phosphatase gene (Wip1) exhibit defects in reproductive organs, immune function, and cell cycle control. Mol Cell Biol 2001;22:1094-105. doi: 10.1128/MCB.22.4.1094-1105.2002.
23. Borst O, Ochmann C, Schönberger T, Jacoby C, Stellos K, Seizer P, *et al*. Methods employed for induction and analysis of experimental myocardial infarction in mice. Cell Physiol Biochem 2011;74:417-22. doi: 10.1159/000331708.
24. Zhu YH, Bulavin DV. Wip1-dependent signaling pathways in health and diseases. Prog Mol Biol Transl Sci 2012;106:307-25. doi: 10.1016/B978-0-12-396456-4.00001-8.
25. Lu X, Nguyen TA, Moon SH, Darlington Y, Sommer M, Donehower LA. The type 2C phosphatase Wip1: An oncogenic regulator of tumor suppressor and DNA damage response pathways. Cancer Metastasis Rev 2008;27:123-35. doi: 10.1007/s10555-008-9127-x.
26. Le Guezennec X, Bulavin DV. WIP1 phosphatase at the crossroads of cancer and aging. Trends Biochem Sci 2010;35:109-14. doi: 10.1016/j.tibs.2009.09.005.
27. Armata HL, Chamberland S, Watts L, Ko HJ, Lee Y, Jung DY, *et al*. Deficiency of the tumor promoter gene wip1 induces insulin resistance. Mol Endocrinol 2014;29:28-39. doi: 10.1210/me. 2014-1136.
28. Du J, Shen X, Zhao Y, Hu X, Sun B, Guan W, *et al.* Wip1-deficient neutrophils significantly promote intestinal ischemia/reperfusion injury in mice. Curr Mol Med 2015;15:100-8. doi: 10.2174/1566524015666150114122929.
29. Frangogiannis NG. Regulation of the inflammatory response in cardiac repair. Circ Res 2012;110:159-73. doi: 10.1161/CIRCRESAHA.111.243162.
30. Nian M, Lee P, Khaper N, Liu P. Inflammatory cytokines and postmyocardial infarction remodeling. Circ Res 2004;94:1543-53. doi: 10.1161/01.RES.0000130526.20854.fa.
31. Frangogiannis NG. Inflammation in cardiac injury, repair and regeneration. Curr Opin Cardiol 2015;30:240-5. doi: 10.1097/HCO.0000000000000158.
32. Chew J, Biswas S, Shreeram S, Humaidi M, Wong ET, Dhillion MK, *et al.* WIP1 phosphatase is a negative regulator of NF-kappaB signalling. Nat Cell Biol 2009;11:659-66. doi: 10.1038/ncb1873.
33. Maxeiner H, Mufti S, Krehbiehl N, Dülfer F, Helmig S, Schneider J, *et al.* Interleukin-6 contributes to the paracrine effects of cardiospheres cultured from human, murine and rat hearts. J Cell Physiol 2014;229:1681-9. doi: 10.1002/jcp.24613.
34. Fischer P, Hilfiker-Kleiner D. Survival pathways in hypertrophy and heart failure: The gp130-STAT3 axis. Basic Res Cardiol 2007;102:279-97. doi: 10.1007/s00395-007-0658-z.
35. Hilfiker-Kleiner D, Shukla P, Klein G, Schaefer A, Stapel B, Hoch M, *et al.* Continuous glycoprotein-130-mediated signal transducer and activator of transcription-3 activation promotes inflammation, left ventricular rupture, and adverse outcome in subacute myocardial infarction. Circulation 2010;122:145-55. doi: 10.1161/CIRCULATIONAHA.109.933127.
36. Dawn B, Xuan YT, Guo Y, Rezazadeh A, Stein AB, Hunt G, *et al.* IL-6 plays an obligatory role in late preconditioning via JAK-STAT signaling and upregulation of iNOS and COX-2. Cardiovasc Res 2004;64:61-71. doi: 10.1016/j.cardiores.2004.05.011.
37. Fuchs M, Hilfiker A, Kaminski K, Hilfikerkleiner D, Guener Z, Klein G, *et al*. Role of interleukin-6 for left ventricular remodeling and survival after experimental myocardial infarction. FASEB J 2003;23:86-91. doi: 10.1096/fj.03-0331fje.

Supplement Table 1: Number of mice used for each experiment

Experiments	WT sham (*n*)	*Wip1*-KO sham (*n*)	WT MI (*n*)	*Wip1*-KO MI (*n*)
Figure 1b: *Wip1* mRNA expression	6	6	6	6
Figure 2a: Survival	8	8	24	35
Figure 2c-2d: Echocardiographic examinations	10	15	10	15
Figure 3a and 3b: Hematoxylin-eosin staining	6	6	6	6
Figure 4a-4c: Body weight, heart weight, and HW/BW ratio	10	10	10	10
Figure 4d and 4e: Wheat germ agglutinin staining	6	6	6	6
Figure 5a: Masson's trichrome staining	6	6	6	6
Figure 5b: Collagen I mRNA expression	6	6	6	6
Figure 6a: *IL-6* mRNA expression	6	6	6	6
Figure 6b: *TNF-α* mRNA expression	6	6	6	6
Figure 6c: *IL-1β* mRNA expression	6	6	6	6
Figure 6d and 6e: p-stat3/stat3	6	6	6	6

WT: Wild-type mice; *Wip1*-KO: Wild-type p53-induced phosphatase 1-knockout mice; MI: Myocardial infarction; HW/BW: Heart weight/body weight; *IL-6*: Interleukin-6; *TNF-α*: Tumor necrosis factor-α; *IL-1β*: Interleukin-1β; stat3: Signal transducers and activators of transcription 3; p-stat3:phosphor-stat3.